Towards an improved description of carbonaceous particle morphology

A. Nobili*, M. Pelucchi*, A. Frassoldati*, T. Faravelli*
tiziano.faravelli@polimi.it
**CRECK Modeling Lab, Department of Chemistry, Materials and Chemical Engineering "G. Natta", Politecnico di Milano, P.zza Leonardo da Vinci 32, 20133 Milano, Italy.*

Abstract
Carbon nanoparticle (CNP) formation from hydrocarbon combustion is of high interest not only for the study of pollutant (soot) emissions, but also in the area of advanced materials. CNP optical and electronical properties, relevant for practical applications, significantly change with their morphology and nanostructure. This work extends a detailed soot kinetic model, based on the discrete sectional approach, to explicitly incorporate the description of CNP polydispersity, maintaining the CHEMKIN-like format. The model considers various nanosized primary particles, generated from liquid-like counterparts through the carbonization process. The model is validated against literature experiments from 11 laminar flames, in both premixed and counterflow configuration, over a wide range of operating conditions (P=1–5 atm, T_{max}=1556-2052 K). The model captures the measured trends of the analyzed CNP properties. Model deviations from the experiments are also discussed.

Introduction
Recent scientific research is driving a paradigm shift on carbonaceous nanoparticles (CNPs) produced from hydrocarbon combustion, looking more and more often at them as attractive materials for new practical applications rather than as harmful pollutants [1].
The strong variation of CNP physical and chemical characteristics as their size and nanostructure evolve in flames was highlighted in several studies. Their size-specific electronic and optical properties were measured and modeled [2], demonstrating the variation of ionization energies and optical band gaps with particle diameter. Regarding CNP morphology, it is known that polydisperse aggregates are formed by primary particles of different sizes [3]. Great efforts have been made to develop kinetic models that can describe this polydispersity in flames. For example, Thomson and coworkers [4] developed an advanced sectional model, based on the solution of transport equations for the number density of aggregates and primary particles. Kraft and coworkers [3] proposed a detailed population balance model (PBM), which describes the evolution of carbonaceous particles by solving the Smoluchowski equation [5]. These models were successfully applied in both one and two-dimensional flame simulations to predict several soot measurements.
This work presents the first discrete sectional model fully written in CHEMKIN format able to predict CNP morphology in terms of primary particle diameter (D_{pp})

profiles, particle size distribution (PSD) and H/C ratio along 1D laminar flames. One of the main advantages of the proposed model is that neither the solution of many additional equations other than those for mass, energy, momentum, and species, nor post-processing steps of numerical results obtained through simplified methods are required. Moreover, the proposed model allows to account for the different reactivity of aggregates that share equivalent mass but possess different surface areas due to the presence of primary particles of different sizes.

Kinetic model

The main features of the discrete sectional model developed by the CRECK modeling group were described in previous works [4]. Large PAHs and CNPs are discretized into 25 sections of lumped pseudo species, called BINs, from 20 to over 10^8 C-atoms. Based on a recent theoretical study on large PAHs [5], aromatic species with >100 C-atoms are modeled as persistent radicals.

In this work, the assumption of primary particles (BIN12, D_p=10 nm) with a single fixed size, adopted in previous versions of the model [4,6], is removed to account for polydispersity. This enables an improved description of the morphology and in turn of the surface reactivity of carbonaceous particles. Carbonaceous particles are distinguished between liquid-like particles (BIN-L) and solid primary particles with an onion like nanostructure (BIN-PP), as shown in Fig. 1. Once the first liquid-like particles (BIN5, D_p=2 nm) form through inception of gas-phase large PAHs, they can Coalesce or Grow ("C&G") towards larger BIN-L (vertical arrows in Fig. 1) or undergo carbonization from Liquid to Solid ("LtoS") primary particles BIN-PP (horizontal arrows in Fig. 1). Indeed, it was experimentally observed that incipient particles are liquid-like amorphous carbonaceous materials [7]. Then, an interplay of physicochemical phenomena governs the transition from liquid-like to solid particles. This transition is driven by the carbonization process. Dobbins [7] proposed a first-order Arrhenius rate constant for the conversion of CNP precursors to carbonaceous species in diffusion flames of eight different hydrocarbon fuels. This rate is here used as reference to model particle carbonization.

Primary particles can then form larger BIN-PP through coagulation and growth (vertical arrows in Fig. 1) or Aggregate ("A") into fractals (diagonal arrows in Fig. 1). The combination of primary particles of different size within the same aggregate would result in an enormous number of BINs. To limit the total number of species in the proposed model, each primary particle is assumed to aggregate forming monodisperse entities, with a fractal dimension D_f = 1.8 [8]. Different monodisperse aggregates (e.g., BIN-AG-I, BIN-AG-II) with equal mass are considered in the model (Fig. 1).

The reference rate parameters for aggregation of solid particles and aggregates are adapted from previous versions of the model [4,6]. The collision efficiency (γ) proposed in [6] is considered to account for the temperature, particle H/C ratio and size dependency of aggregation reactions. For coalescence, which involves at least one liquid-like particle (BIN-L), different rates are considered. In particular, a

unitary collision efficiency ($\gamma = 1$) is assumed. Moreover, based on the molecular dynamic (MD) simulations performed in [9], coalescence rates are scaled with respect to the volume ratio of the colliding entities.

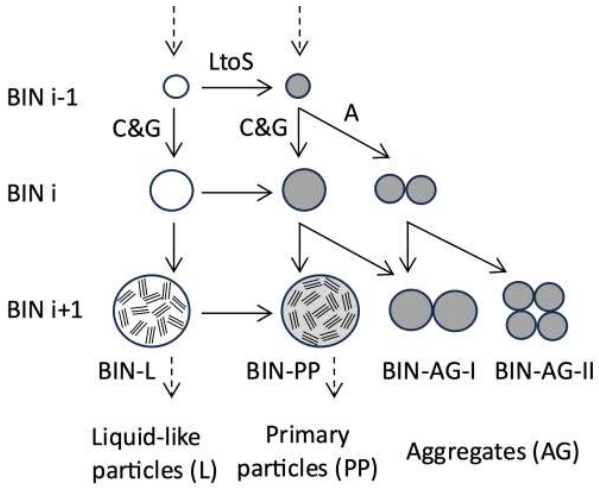

Figure 1. Schematic representation of the polydisperse CRECK model. The arrows represent different reaction classes: carbonization, i.e., the transition from liquid to solid particles ("LtoS"), coalescence and surface growth ("C&G"), and aggregation ("A").

Reaction classes for inception, surface growth, dehydrogenation and oxidation with their reference rate parameters are taken from previous versions of the CRECK model [4,6]. The overall model, coupled with detailed gas-phase chemistry up to 5-ring aromatics [6] and it is fully written in CHEMKIN format. Numerical simulations are carried out with the OpenSMOKE++ framework [10].

Results and discussion

Model validation is performed by comparison with data from 11 laminar flames, whose operating conditions are summarized in Table 1. The selected flames include three different configurations: premixed flat flames established on the McKenna-type burner (LPF), premixed burner-stabilized stagnation flames (BSSF) and counterflow diffusion flames (CFDF).

The series of premixed ethylene flames experimentally studied by Xu and Faeth [11] and the series of counterflow diffusion ethylene flames by Amin et al. [12] are selected to assess the model performances against literature data of average primary particle diameter (D_{pp}), at different equivalence ratios (ϕ = 2.34-2.94) and pressures (P = 2-5 atm) in the premixed and in the counterflow configuration, respectively.

In the series of premixed flames, the model captures the increase of average primary particle diameter (Fig. 2a) as the equivalence ratio increases. A good quantitative agreement between measurements and simulations is obtained for both carbonaceous particle properties at ϕ = 2.34 and 2.64, while larger deviations occur at ϕ = 2.94.

Table 1. Laminar flames investigated.

#Flame	Type	T_{max}, K	P, atm	$^{*}\phi/^{**}Z_{st}$	$^{*}v_0$, cm $s^{-1}/^{**}K_G$, s^{-1}	L, mm	Ref.
F1	LPF	1644	1	2.34	6.8	30	[11]
F2	LPF	1600	1	2.34	6.8	30	[11]
F3	LPF	1556	1	2.34	6.8	30	[11]
F4	CFDF	1983	2	0.17	30	8.2	[12]
F5	CFDF	2016	3	0.17	30	8.2	[12]
F6	CFDF	2037	4	0.17	30	8.2	[12]
F7	CFDF	2052	5	0.17	30	8.2	[12]
F8	BSSF	1783	1	2.06	8	5	[13]
F9	BSSF	1832	1	2.06	8	10	[13]
F10	LPF	1700	1	2.40	4	14	[14]
F11	LPF	1770	1	2.40	5	16	[14]

*Equivalence ratio (ϕ) and cold gas velocity (v_0) for premixed flames. **Stoichiometric mixture fraction (Z_{st}) and global strain rate (K_G) for counterflow flames.

The evolution of D_{pp} profiles along the axial coordinate of the flame at different equivalence ratios is well reproduced, with maximum deviations by a factor of ~1.2 at ϕ = 2.94. Importantly, Fig. 2a shows the improved predictive capability of the proposed model, which accounts for CNP polydispersity, with respect to its previous version [4], which instead assumes monodisperse aggregates constituted by fixed size primary particles (D_{pp}=10 nm, red dashed line in Fig. 2a).
In the series of counterflow flames F4-F7, the polydisperse model also captures the increase of D_{pp} (Fig. 2b). However, the measured peak D_{pp} is characterized by a more pronounced increase from 2 to 5 atm, i.e., from 13 to 52 nm, respectively, compared to the model predictions, i.e., from 28 to 40 nm. Moreover, the model predicts a steeper increase of the D_{pp} profiles from ~0.45 cm from the fuel nozzle toward the particle stagnation plane, where the larger primary particle diameters are reached. On the other hand, the model captures the increasing slope of the D_{pp} profiles from 2 to 5 atm as well as the shift of the peak D_{pp} location towards larger distances from the fuel nozzle as pressure increases (Fig. 2b).
Another key morphological property of CNPs is the particle size distribution (PSD). The PSD measurements of Shao et al. [13], performed in a series of BSS ethylene flames (F8-F9 in Table 2) at different height above the burner (H_p) are selected to analyze the related model predictions (Fig. 2c). The proposed model satisfactorily describes the transition from the unimodal to the bimodal distribution with the increase of particle residence time from H_p = 5 mm to 10 mm. The clear development of the throat at H_p = 10 mm obtained with the proposed model represents another relevant improvement in the description of the PSD evolution with respect to its previous version [6], which considers neither CNP polydispersity nor the scaling of coalescence rates with the volume ratio of the colliding entities described above.

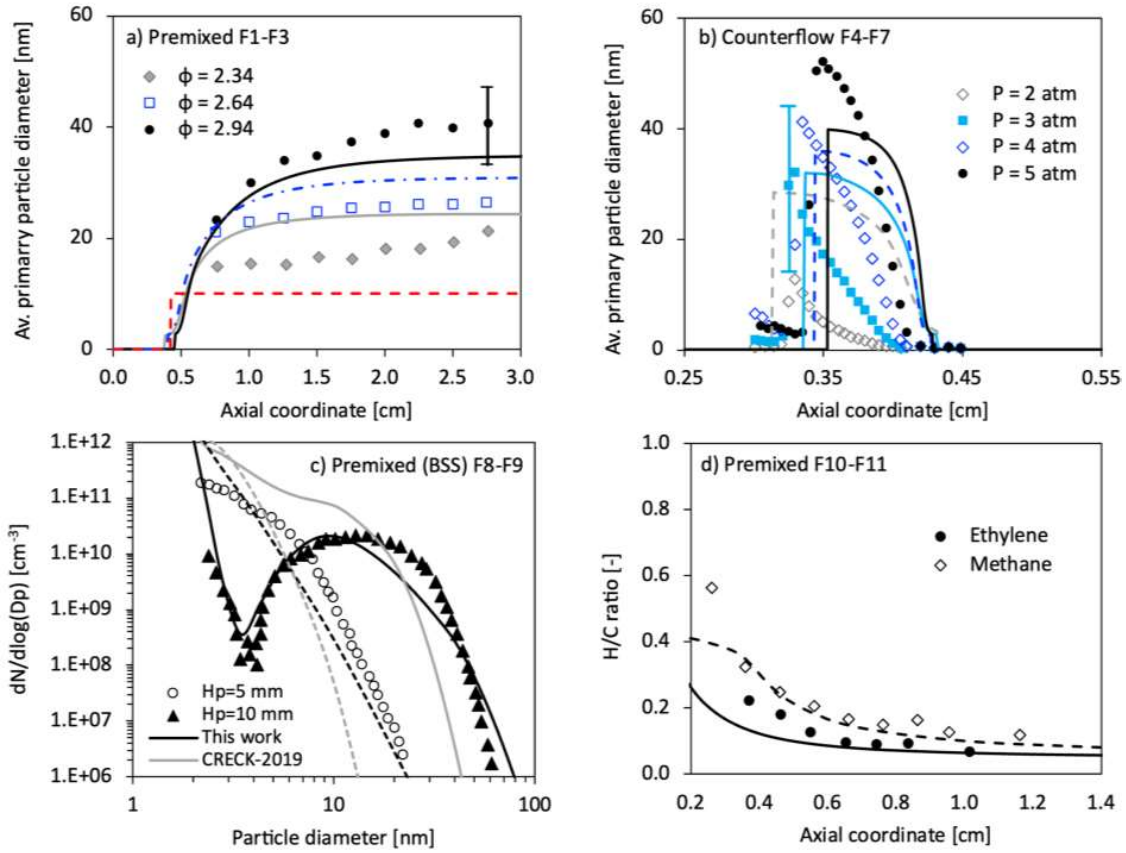

Figure 2. Average primary particle diameter profiles in a) laminar ethylene premixed (F1-F3) [11] and b) counterflow flames (F4-F7) [12]. Particle size distribution at H_p=5 and 10 mm in BSS ethylene flames (F8-9) [13]. H/C ratio profiles in ethylene (F10) and methane (F11) premixed flames [14]. Symbols: experiments; lines: model simulations.

Finally, the model is validated against experimental data of particle H/C ratio in two laminar premixed flames fueled by ethylene and methane by Russo et al. [14]. Model simulations well capture the formation of more dehydrogenated carbonaceous particles in the ethylene flame (F10) with respect to those produced in the methane flame (F11), due to the related lower fuel H/C ratio (2 for C_2H_4 and 4 for CH_4). These results highlight the good model description of carbonaceous nanostructure, which significantly determines not only the reactivity [2] but also the optical and electronic properties of CNPs, as discussed in the introduction of this work.

Conclusions

A novel detailed discrete sectional model for CNP formation has been presented in this work. The main novelty introduced is the description of CNP polydispersity achieved by considering the formation of primary particles with different sizes from liquid-like counterparts through the carbonization process. Compared to previous versions of the model, this allows to predict the evolution of average primary particle diameters (D_{pp}) measured in both premixed and counterflow diffusion ethylene flames. The model also captures the measured trends of particle size distribution

(PSD) and particle H/C ratio. Future studies are necessary to perform more accurate rate estimation of key processes like carbonization, coalescence and aggregation, characterized by the largest uncertainties, but significantly affecting model predictions of CNP morphology.

References

[1] Lindstedt R.P., Michelsen H.A., Mueller M.E., "Special issue and perspective on the chemistry and physics of carbonaceous particle formation", *Combust Flame* 113042 (2023).
[2] Liu C., Singh A. V., Saggese C., Tang Q., Chen D., Wan K., Vinciguerra M., Commodo M., De Falco G., Minutolo P., D'Anna A., Wang H., "Flame-formed carbon nanoparticles exhibit quantum dot behaviors", *Proceedings of the National Academy of Sciences* 116: 12692–7 (2019).
[3] Botero M.L., Eaves N., Dreyer J.A.H., Sheng Y., Akroyd J., Yang W., Kraft M., "Experimental and numerical study of the evolution of soot primary particles in a diffusion flame", *Proceedings of the Combustion Institute* 37: 2047–55 (2019).
[4] Nobili A., Cuoci A., Pejpichestakul W., Pelucchi M., Cavallotti C., Faravelli T., "Modeling soot particles as stable radicals: a chemical kinetic study on formation and oxidation. Part I. Soot formation in ethylene laminar premixed and counterflow diffusion flames", *Combust Flame* 243: 112073 (2022).
[5] Nobili A., Pratali Maffei L., Baggioli A., Pelucchi M., Cuoci A., Cavallotti C., Faravelli T., "On the radical behavior of large polycyclic aromatic hydrocarbons in soot formation and oxidation", *Combust Flame* 111692 (2021).
[6] Pejpichestakul W., Frassoldati A., Parente A., Faravelli T., "Kinetic modeling of soot formation in premixed burner-stabilized stagnation ethylene flames at heavily sooting condition", *Fuel* 234: 199–206 (2018).
[7] Dobbins R.A., "Soot inception temperature and the carbonization rate of precursor particles", *Combust Flame* 130: 204–14 (2002).
[8] Schenk M., Lieb S., Vieker H., Beyer A., Gölzhäuser A., Wang H., Kohse-Höinghaus K., "Morphology of nascent soot in ethylene flames", *Proceedings of the Combustion Institute* 35: 1879–86 (2015).
[9] Hawa T., Zachariah M.R., "Coalescence kinetics of unequal sized nanoparticles", *J Aerosol Sci* 37: 1–15 (2006).
[10] Cuoci A., Frassoldati A., Faravelli T., Ranzi E., "OpenSMOKE++: An object-oriented framework for the numerical modeling of reactive systems with detailed kinetic mechanisms", *Comput Phys Commun* 192: 237–64 (2015).
[11] Xu F., Sunderland P.B., Faeth G.M., "Soot formation in laminar premixed ethylene/air flames at atmospheric pressure", *Combust Flame* 108: 471–93 (1997).
[12] Amin H.M.F., Roberts W.L., "Soot measurements by two angle scattering and extinction in an N2-diluted ethylene/air counterflow diffusion flame from 2 to 5 atm", *Proceedings of the Combustion Institute* 36: 861–9 (2017).
[13] Shao C., Campuzano F., Zhai Y., Wang H., Zhang W., Mani Sarathy S., "Effects of ammonia addition on soot formation in ethylene laminar premixed flames", *Combust Flame* 235: 111698 (2022).
[14] Russo C., Tregrossi A., Ciajolo A., "Dehydrogenation and growth of soot in premixed flames", *Proceedings of the Combustion Institute* 35: 1803–9 (2015).